A Theory of Premelting Dynamics for all Power Law Forces

J. S. Wettlaufer,[1,3] M. G. Worster,[2] L. A. Wilen,[3] and J. G. Dash[3]
[1]*Applied Physics Laboratory, University of Washington, Box 355640, Seattle, Washington 98105*
[2]*Institute of Theoretical Geophysics, Department of Applied Mathematics and Theoretical Physics, University of Cambridge, CB3 9EW Cambridge, England*
[3]*Department of Physics, University of Washington, Box 351560, Seattle, Washington 98195*
(Received 15 January 1996)

We present a new theory for premelting dynamics valid for all power law interfacial free energies, and reexamine recent frost heave dynamics experiments in light of the predictions. We find a family of similarity solutions and examine a subset relevant to several types of interaction. The experimental frost heave data are best described in terms of an electrostatic interfacial free energy. The results are generally important in the dynamics of wetting under interfacial interactions. [S0031-9007(96)00097-X]

PACS numbers: 64.70.Dv, 68.15.+e, 68.45.Gd, 82.65.Dp

The stable existence of interfacial water below the bulk freezing point has been associated with frost heave for decades but the basic causes are only just now being addressed in the context of interfacial premelting [1]. Supercooled liquid of any material is metastable in *bulk* but may find a stable existence at *interfaces*. In the case of H_2O, the mobility and pressure of this liquid can have dramatic effects in the polar and subpolar regions by controlling impurity redistribution within sea and glacier ice [1], weathering rocks and soils [2], and influencing structural design [3]. The main dynamical prediction of premelting thermodynamics [4,5] is that liquid motion in interfacial films is driven by a temperature gradient which induces a chemical potential gradient, driving liquid from high to low temperatures. The phenomenon is possible in any material in which interfacial interactions extend the equilibrium domain of the liquid phase into the solid region of the bulk phase diagram.

Frost heave studies have traditionally been conducted in porous media which have the advantage of greatly increased surface area of premelted liquid. Unfortunately the convolution of curvature, surface disorder, and the tortuosity of the medium obscures the fundamental flow behavior [1], which has only recently been revealed in experimental studies of isolated crystalline interfaces.

In the following we derive the theory germane to a recent experimental study of interfacial dynamics on single crystal facets of ice [6]. A liquid film of melt (ℓ), thickness d, and area A_i may disjoin a solid (s) from a wall at temperatures below the bulk freezing point as the result of the competition between a reduction of interfacial free energy and the expense of maintaining a layer of undercooled liquid [1]. It is properly thought of as a wetting phenomenon away from bulk coexistence (e.g., [7]). The free energy of the system,

$$\Omega = -P_\ell V_\ell - P_s V_s + \mathcal{I}(d), \tag{1}$$

is composed of bulk and surface terms, where P and V denote pressure and volume. The interfacial term $\mathcal{I}(d) = [\Delta\gamma f(d) + \gamma_{sw}]A_i$, where $\Delta\gamma = \gamma_{s\ell} + \gamma_{\ell w} - \gamma_{sw}$, and the γ's are the solid-liquid ($s\ell$), liquid-wall (ℓw), and solid-wall (sw) interfacial free energies, captures the film thickness dependence of the free energy [8]. Melting may be *complete* or *incomplete* [1,9]. Complete interfacial melting occurs when the film thickness diverges as the bulk melting point T_m is approached from below, in which case $\mathcal{I}(d)$ is a positive, monotonically decreasing function of d at long range. Power law interaction potentials have the form $f(d) = 1 - (\sigma/d)^n$, where σ is on the order of a molecular diameter, and n depends on the nature of the interactions. In incomplete interfacial melting the film growth is truncated at finite undercooling. The minimization of Ω at fixed temperature and chemical potential yields two results [8]. First, a pressure difference between the melt film and the solid,

$$P_\ell - P_s = \Delta\gamma n \sigma^n d^{-(n+1)}, \tag{2}$$

is a general result. Second, to first order in the reduced temperature $t_r = (T_m - T)/T_m$, the film thickness is

$$d = \left(-\frac{(\nu-1)\sigma^{\nu-1}\Delta\gamma}{\rho_s q_m}\right)^{1/\nu} t_r^{-1/\nu} \equiv \lambda_\nu t_r^{-1/\nu}, \tag{3}$$

where $\nu = n + 1$, ρ_s is the density of the solid, and q_m is the latent heat of fusion [10]. Equation (2) tells us that the pressure is uniform in each phase, but that interfacial interactions create a pressure difference between the melted layer and the bulk solid, and Eq. (3) shows that the film thickens with temperature. The essential idea of premelting dynamics can be described by combining these two results,

$$P_\ell = P_s - \rho_s q_m t_r\ . \tag{4}$$

Suppose we fix P_s, then the pressure in the film, P_ℓ, must increase with temperature. Therefore, a temperature gradient parallel to a premelted interface will drive a flow in the film toward lower temperatures [11]. Because

 0031-9007/96/76(19)/3602(4)$10.00

the film thins as the temperature decreases, continuity demands that liquid will convert to solid as it moves toward lower temperatures.

Wilen and Dash [6] have studied the motion of a water layer in a temperature gradient, $\mathcal{G}$, at the interface between a single crystal of ice and a flexible polymer membrane. Spatial gradients in the thin-film volume flux lead to the growth of the solid, causing changes in the height of the membrane, $h = h(x,t)$, measured relative to an initial reference height $h(x,t_0)$. They found that flow occurred in a narrow range of temperature near T_m. At lower temperatures, the *relative* lack of membrane deformation was interpreted as an abrupt decrease to $d = 0$, consistent with an interfacial free energy that decreases monotonically with film thickness at long range, but which possesses a local minimum at shorter range. The underlying dynamics of frost heave are controlled by the nature of the intermolecular interactions in the system *and* the mechanical interaction between the film and the membrane. Here, we uncover the relationship between these two controlling factors.

The radial cell configuration can be treated in a one-dimensional slab geometry (Fig. 1) since the membrane height deformations are much less than the disk radius. The flow is driven by a thermomolecular pressure gradient,

$$\nabla P_\ell = -\rho_\ell q_m \nabla t_r + \frac{\rho_\ell}{\rho_s}\nabla P_s\,, \tag{5}$$

where P_s is the external pressure exerted on the solid by the membrane [1,6,8,12]. The relaxation time of the film to the thickness determined by Eq. (3) is negligible relative to that for heat conduction. Mass conservation is written as

$$\partial_t h + \partial_x Q = 0\,, \tag{6}$$

where Q is the volume flux per unit breadth through the film of thickness given by Eq. (3), and for a lubrication flow it is

$$Q = -\frac{d^3}{12\mu}\nabla P_\ell\,, \tag{7}$$

where μ is the viscosity [8]. The membrane possesses a tension, $\tilde{\sigma}$, and when distorted it exerts a pressure on the solid proportional to the curvature [13]. Combining Eqs. (3)–(7), and noting that $t_r = \mathcal{G}x/T_m$, so that $d^3 \propto x^{-3/\nu}$ yields the following dimensional equation for the evolution of the membrane height:

$$\partial_t h + \Lambda_\nu \partial_x[x^{-3/\nu}(1 + \alpha h_{xxx})] = 0\,, \tag{8}$$

where

$$\alpha = \frac{\tilde{\sigma}T_m}{\rho_s q_m \mathcal{G}}, \qquad \Lambda_\nu = \frac{\lambda_\nu^3 \rho_\ell q_m}{12\mu}\left(\frac{T_m}{\mathcal{G}}\right)^{(3-\nu)/\nu}. \tag{9}$$

Analysis of Eq. (8) suggests the following similarity solution:

$$h = \alpha^{-1}(\Lambda_\nu \alpha t)^{3\nu/(4\nu+3)} f(\eta)\,, \tag{10}$$

with similarity variable

$$\eta = x(\Lambda_\nu \alpha t)^{-\nu/(4\nu+3)}. \tag{11}$$

This leads to a family of fourth-order, dimensionless ordinary differential equations for the function $f(\eta)$,

$$f'''' = \frac{3}{\nu}\frac{f''' + 1}{\eta} + \frac{\nu}{4\nu + 3}\eta^{(3/\nu)+1} f' - \frac{3\nu}{4\nu + 3}\eta^{3/\nu} f\,, \tag{12}$$

where the primes denote $d/d\eta$. Note that there are no free parameters in Eq. (12). The experimental cell is large enough so that the membrane height is unaffected by the edges [6], and the cell center ($\eta = \eta_c$) is far from the region of deformation, suggesting the following boundary conditions:

$$f' = f'' = 0 \qquad (\eta = 0) \quad \text{and} \quad f' = 0 \qquad (\eta = \eta_c)\,. \tag{13}$$

As $\eta \to \infty$ asymptotic analysis of Eq. (12) reveals that the membrane height decays algebraically as

$$f \sim \eta^{-[3/(\nu+1)]} \qquad (\eta \to \infty)\,. \tag{14}$$

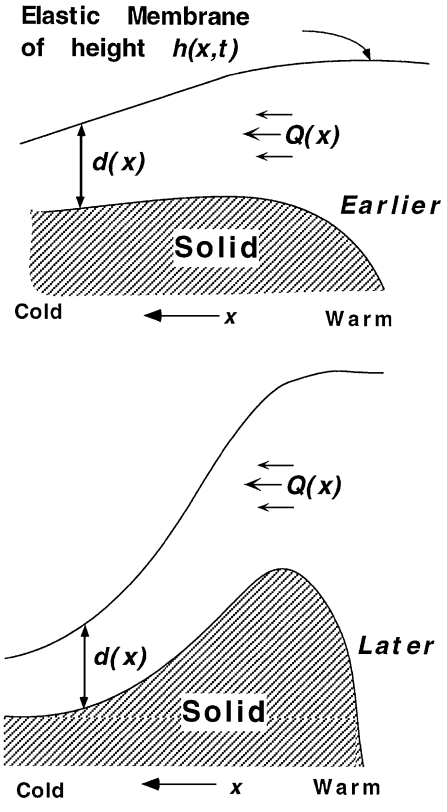

FIG. 1. The local configuration of the system. The temperature gradient $\mathcal{G}$ is constant so $t_r = \mathcal{G}x/T_m$, and the film thickness d depends only on x. Volume flux gradients $\partial_x Q$ drive the evolution of the membrane height $h(x,t)$ relative to an initial reference height $h(x,t_0)$.

Finally, a necessary condition on the solution is that

$$f''' = -1 \qquad (\eta = 0). \tag{15}$$

Equation (12) subject to (13)–(15) was solved numerically using a finite-difference method that exploits an adaptive mesh and collocation at Gaussian points.

In Fig. 2 we show the cases where the premelting behavior was dominated by electrostatic ($\nu = 3/2, 2$), nonretarded ($\nu = 3$), and retarded ($\nu = 4$) van der Waals interactions. By electrostatic interfacial interactions we refer to a simple treatment in which the substrate possesses a surface charge density and the confinement of counterions present in the liquid layer creates a repulsive interaction [9]. We can approximate $\mathcal{I}(d) \propto d^{-1/2}$, over a reasonable range for small d, and at long range $\mathcal{I}(d) \propto d^{-1}$ [9]. Two features that are independent of the nature of the interactions are (a) the membrane deformation takes a maximum value in the region of the high temperatures where the film thickness and the gradient in the volume flux are maximal and (b) there is an infinite train of oscillations with an exponentially decaying amplitude about the algebraically decaying mean value of f [cf. Eq. (14)]. The elasticity induced curvature, that was not considered in an earlier theory [8], is responsible for the secondary maxima as follows. The primary maximum creates a positive curvature which the elasticity of the membrane attempts to straighten out. As it does so it draws fluid in *from* both the high and low temperature regions. The fluid drawn from low temperatures creates the first trough, which the membrane again tries to straighten and thereby pushes fluid away *toward* both the high and low temperature regions. The fluid pushed toward low temperatures creates the second peak, and so on *ad infinitum* .

At any time Eqs. (10) and (11) show that f' describes dh/dx for a given interaction. The slope of the membrane is maximal in the ($\nu = 3/2$) electrostatic case, and the first minimum and secondary maximum are found at higher temperatures and are more localized in space. This can be understood by noting that the volume flux is a product of the film thickness cubed and the thermomolecular pressure gradient, seen as $x^{-3/\nu}$ and $1 + \alpha h_{xxx}$ in Eq. (8). The former depends on the nature of the interactions and, as has been shown previously (e.g., [1]), the latter is a universal thermodynamic statement. The membrane deformation is driven by the gradient of this product; as the exponent ν characterizing the interactions *decreases*, the decay in the volume flux *increases*, thereby localizing frost heave as is seen in Fig. 2.

The most robust experimental feature is the time evolution of the maximum height $h_{\max}$ of the membrane. Equation (10) predicts the scaling

$$h_{\max} = \alpha^{-1}(\Lambda_\nu \alpha t)^{3\nu/(4\nu+3)} f_{\max}. \tag{16}$$

The coefficient depends only on material constants multiplied by $[(\nu - 1)\sigma^{\nu-1}\Delta\gamma]^{-[9/(4\nu+3)]}$, which we fit to determine the slope of the interfacial potential $\mathcal{I}(d)$. For example, when $\nu = 3$ we are estimating the Hamaker constant [10]. The fits span several decades in time (Fig. 3). The coefficient for a given interaction then allows us to predict $h(x, t)$ by solving the relevant evolution equation [from Eqs. (12)]. The agreement between theory and experiment (Fig. 4) is best in the case of electrostatic interactions which always dominate van der Waals at long range and, depending on the surface charge density, may also dominate at short range [9].

It is clear that the van der Waals interaction does not dominate the melting behavior. Less certain is that an electrostatic interaction is solely responsible for the observed behavior. Since the latter dominates at long range [9], we have confidence in the calculation for the region where the heave is maximal, but this does not exclude the role of other interactions. A crossover with temperature from one type of interaction to another can be treated, but will not be describable by a similarity solution. Since the height

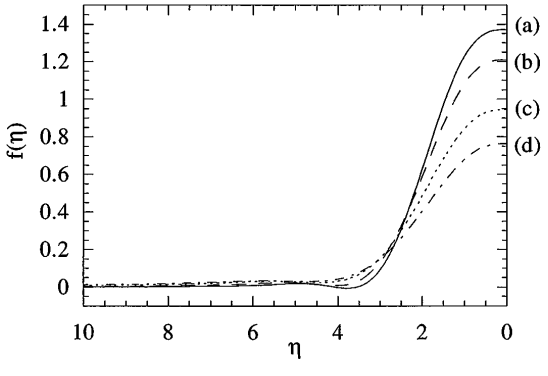

FIG. 2. Plot of the similarity solutions for the dimensionless membrane height f as a function of the similarity variable η, in the cases where the interfacial free energies describe (a) and (b) electrostatic ($\nu = 3/2$) and ($\nu = 2$), (c) nonretarded ($\nu = 3$) and (d) retarded ($\nu = 4$) van der Waals interactions.

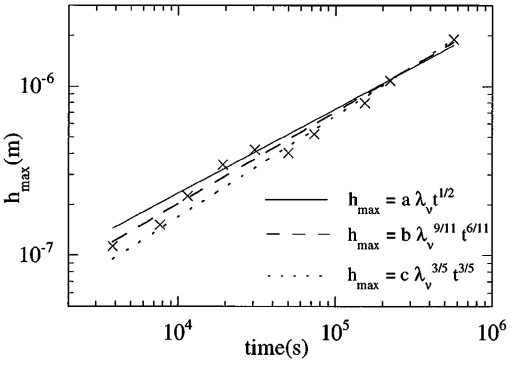

FIG. 3. Three fits of the maximum height of the membrane $h_{\max}(t)$ as given by Eq. (16). The $t^{1/2}$, $t^{6/11}$, and $t^{3/5}$ power laws arise from the short and long range electrostatic ($\nu = 3/2$ and $\nu = 2$) and nonretarded van der Waals ($\nu = 3$) interactions, respectively. The parameter that is fitted for each interaction is $[(\nu - 1)\sigma^{\nu-1}\Delta\gamma]^{-[9/(4\nu+3)]}$, related to λ_ν as defined in Eq. (3). a, b, and c are completely determined material constants, and $\lambda_{\nu=3/2} = 0.0337$ Å, $\lambda_{\nu=2} = 0.2101$ Å, and $\lambda_{\nu=3} = 1.3759$ Å.

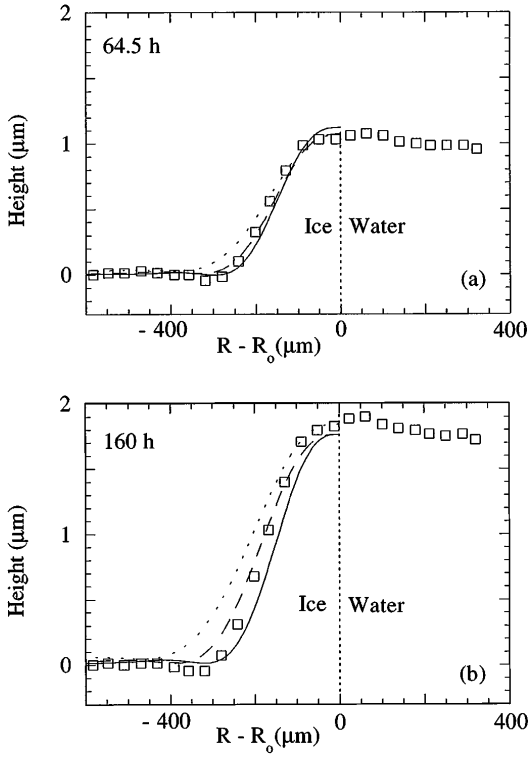

FIG. 4. Comparsion between the theoretical predictions and the experimental values described in [6] for $h(x,t)$ at (a) 64.5 and (b) 160 h. $R - R_o$ is the experimental x coordinate. At the *bulk* ice/water interface ($R = R_o$) $\mathcal{G} = 0.92\ \mathrm{K\,cm^{-1}}$. The predictions for the short and long range electrostatic ($\nu = 3/2$ and $\nu = 2$), and the nonretarded van der Waals ($\nu = 3$) interactions are shown by the solid, dashed, and dotted lines, respectively. "Ice" ($R - R_o < 0$) and "water" ($R - R_o > 0$) refer to regions where the *bulk* phases are stable. For $R - R_o < 0$ an *interfacial* water film coexists between the membrane and *bulk* ice.

grows a thousand times faster than it spreads [Eqs. (10) and (11)], the relative deformation at lower temperatures is so small we expect that the secondary maxima, for any type of interaction, and distinctions between different interactions in that region will severely test experimental resolution. The scaling clearly exhibits that varying the temperature gradient may allow these subtle features to be extracted.

The most important result concerns a new interpretation of the experimental data. The *relative* lack of membrane deformation at lower temperatures was interpreted as an abrupt decrease to $d = 0$, consistent with an interfacial free energy that decreases monotonically with film thickness at long range, but which possesses a local minimum at shorter range. Here we have shown that the experimental data can be described with an interfacial free energy that decreases monotonically over the entire range of film thicknesses.

Interesting issues associated with proximity effects [1] await understanding. From the theoretical perspective the results are of fundamental interest in other lubrication flows where the equations of motion possess scaling behavior [14]. Since experimental verification of similarity solutions over the time scales shown here is rare, we hope that our theory stimulates further experimentation.

It is a pleasure to acknowledge extremely useful conversations with M. P. Brenner, J. W. Cahn, J. F. Nye, H. A. Stone, and S. C. Fain. This work has been generously supported by Grants No. ONR N00014-90-J-1369, No. N00014-91-1-0120, No. NSF DPP 90-23845, and No. DMR 94-00637.

[1] J. G. Dash, H.-Y. Fu, and J. S. Wettlaufer, Rep. Prog. Phys. **58**, 115 (1995).

[2] J. Walder and B. Hallet, Geol. Soc. Am. Bull. **96**, 336 (1985).

[3] P. J. Williams and M. W. Smith, *The Frozen Earth: Fundamentals of Geocryology* (Cambridge University Press, Cambridge, 1989).

[4] J. G. Dash, in *Proceedings of the Nineteenth Solvay Conference*, edited by F. W. de Wette (Springer-Verlag, Berlin, 1988); Science **246**, 1591 (1989).

[5] H. Löwen, T. Beier, and H. Wagner, Europhys. Lett. **9**, 791 (1989); R. Lipowsky *et al.*, Phys. Rev. Lett. **62**, 913 (1989).

[6] L. A. Wilen and J. G. Dash, Phys. Rev. Lett. **74**, 5076 (1995).

[7] M. Schick, in *Liquids at Interfaces, Les Houches Session XLVIII*, edited by J. Charvolin, J. F. Joanny, and J. Zinn-Justin (Elsevier, New York, 1990), p. 415; S. Dietrich, in *Phase Transitions and Critical Phenomena*, edited by C. Domb and J. Lebowitz (Academic, New York, 1988), Vol. 12.

[8] J. S. Wettlaufer and M. G. Worster, Phys. Rev. E **51**, 4679 (1995).

[9] L. A. Wilen, J. S. Wettlaufer, M. Elbaum, and M. Schick, Phys. Rev. B **52**, 12 426 (1995). See Fig. 5 where $\mathcal{I}(d)$ is plotted for various surface charge densities.

[10] For $\nu = 3$, $\sigma^2 \Delta\gamma = A/12\pi$; A is the Hamaker constant (e.g., see Appendix of [8]), but clearly the coefficient of λ_ν depends on ν.

[11] This is (a) equivalent to a gradient in the *disjoining pressure* along a wetting substrate, e.g., P. G. de Gennes, Rev. Mod. Phys. **57**, 827 (1985); L. Leger and J. F. Joanny, Rep. Prog. Phys. **55**, 431 (1992), or (b) analogous to the creeping He film which experiences a spatially varying body force; J. N. Israelachvili, *Intermolecular and Surface Forces* (Academic Press Inc., London, 1992).

[12] R. R. Gilpin, Water Resour. Res. **16**, 918 (1980).

[13] The membrane energy is dominated by surface tension: $\tilde{\sigma} = 1\ \mathrm{psi\,cm^{-1}}$, Young's modulus $E \approx 600$ psi and the membrane is 0.025 mm thick, so that the bending energy contributes only about 1% to the membrane energy. Furthermore, the radius of curvature is large compared to d, so the membrane exerts a pressure deep within the solid. Although the solid can maintain a shear stress, we assume that any plastic deformation is slow relative to the film dynamics.

[14] A. L. Bertozzi, M. P. Brenner, T. F. Dupont, and L. P. Kadanoff, in *Trends and Perspectives in Applied Mathematics*, edited by L. Sirovich, Applied Mathematical Sciences Vol. 100 (Springer-Verlag, New York, 1994), p. 155.